Am J Nucl Med Mol Imaging 2018;8(5):351-359
www.ajnmmi.us /ISSN:2160-8407/ajnmmi0082704

Original Article

^{68}Ga-PSMA-11 PET/CT in prostate cancer local recurrence: impact of early images and parametric analysis

Christos Sachpekidis[1,2], Leyun Pan[1], Boris A Hadaschik[3,4], Klaus Kopka[5,6], Uwe Haberkorn[1,2], Antonia Dimitrakopoulou-Strauss[1]

[1]Clinical Cooperation Unit Nuclear Medicine, German Cancer Research Center (DKFZ), Heidelberg, Germany; Departments of [2]Nuclear Medicine, [3]Urology, University Hospital Heidelberg, Heidelberg, Germany; [4]Department of Urology, University Hospital Essen, Essen, Germany; [5]Division of Radiopharmaceutical Chemistry, German Cancer Research Center (DKFZ), Heidelberg, Germany; [6]German Cancer Consortium (DKTK), Heidelberg, Germany

Received July 17, 2018; Accepted August 24, 2018; Epub October 20, 2018; Published October 30, 2018

Abstract: ^{68}Ga-PSMA-11 PET/CT performed 60 min post tracer injection (p.i.) can underestimate prostate cancer (PC) local recurrence, due to high ^{68}Ga-PSMA-11 urinary bladder accumulation. Aim of this analysis is to evaluate the complementary role of early dynamic and parametric PET imaging in patients with PC local recurrence. Sixteen patients with PC biochemical relapse attributed to local recurrence underwent dynamic ^{68}Ga-PSMA-11 PET/CT scanning of the pelvis and whole-body PET/CT. Data analysis was based on visual analysis of the PET/CT scans, SUV calculations, quantitative analysis based on two-tissue compartment and Patlak models as well as parametric imaging based on Patlak analysis. 12/16 patients were PSMA-positive in the static ^{68}Ga-PSMA-11 PET/CT scans (60 min p.i.). All 12 lesions corresponding to PC local recurrence were detected in the early dynamic images at a median time of 4.5 min p.i. (range = 1.5-11.5 min). Moreover, early dynamic PET imaging could detect local recurrence in 1/4 static PET/CT-negative patients. Tracer accumulation in the urinary bladder began at a median time of 10 min (range = 6.0-17.5 min). All PC local recurrences visible on late static PET/CT and the local recurrence, which was positive only in early dynamic but not in late PET images, could be delineated on Patlak images. The present findings indicate that early dynamic ^{68}Ga-PSMA-11 PET/CT scan of the pelvis up to 12 min p.i. as well as Patlak analysis, performed in addition to the conventional PET/CT acquired at 60 min p.i., seem a practical approach to increase the detection rate of PC local recurrence.

Keywords: Prostate cancer local recurrence, ^{68}Ga-PSMA-11 PET/CT, early dynamic PET imaging, Patlak analysis

Introduction

Biochemical recurrence occurs in up to 40% of prostate cancer (PC) patients after radical prostatectomy [1]. Accurate localization of relapsing disease at low prostate specific antigen (PSA) levels is of significance, because the subsequent application of early salvage radiotherapy provides a possibility of cure. In particular, it is expected that more than 60% of patients being treated before the PSA level rises to >0.5 ng/ml, will achieve an undetectable PSA level [2]. Despite the significant advances that have taken place especially in the field of magnetic resonance imaging (MRI), conventional imaging modalities still have clear limitations in PC recurrence assessment [1, 2].

Positron emission tomography/computed tomography (PET/CT) with the ^{68}Ga-labelled prostate specific membrane antigen (PSMA) Glu-urea-Lys-(Ahx)-HBED-CC (^{68}Ga-PSMA-11) has emerged in the current decade as a novel imaging modality with proven clinical value in PC biochemical recurrence management [5-7]. Nevertheless, when performed with the 'conventional' protocol of static image acquisition at 60 min post tracer injection, the modality carries the inherent disadvantage of high ^{68}Ga-PSMA-11 accumulation in the bladder,

which can mask the detection of PC local recurrence [8].

Dynamic PET/CT (dPET/CT) allows registration of pharmacokinetic information over time, unlike classical PET/CT protocols that enable the acquisition of patient images only at one time point after tracer injection. With the application of compartment modeling as well as parametric image analysis of the dPET data, different features of the tracer kinetics can be visualized. In an attempt to increase the diagnostic efficacy of ^{68}Ga-PSMA-11 PET/CT, we aimed in the present study to evaluate the complementary role of early dynamic and parametric PET imaging in patients with local recurrence of PC.

Materials and methods

Patients

16 patients with biochemical relapse of PC attributed to local recurrence, based on imaging (MRI, PET/CT with ^{68}Ga-PSMA-11) findings, were enrolled in this retrospective analysis. All patients had undergone primary therapy with curative intent. Their median age was 69.5 years (range = 57-78 years). The median PSA value was 2.4 ng/mL (range = 0.2-19.9 ng/mL). Gleason score was available in 12/16 patients (median = 7.5; range = 6-10). **Table 1** presents the characteristics of the patients investigated. The analysis was conducted in accordance to the declaration of Helsinki with approval of the ethical committee of the University of Heidelberg and the federal agency of radiation protection.

Data acquisition

The patients were intravenously administered with ^{68}Ga-PSMA-11, which was synthesized and radiolabeled as published previously [9, 10]. Data acquisition consisted of two parts: the dynamic part (dPET/CT studies) and the static part (whole body PET/CT). dPET/CT studies were performed over the pelvic area and the lower abdomen (two bed positions, 44 cm) for 60 min using a 24-frame protocol (10 frames of 30 seconds, 5 frames of 60 seconds, 5 frames of 120 seconds and 4 frames of 600 seconds). Whole body static imaging was performed in all patients with an image duration of 2 min per bed position for the emission scans after the end of the dynamic acquisition. Details regarding data acquisition are described in previous publications of our group [11-13].

Data analysis

Data analysis and evaluation was based on visual analysis of the static and dynamic PET/CT scans, volume of interest-based (VOI-based) analysis leading to semi-quantitative (standardised uptake value-SUV) and quantitative calculations based on a two-tissue compartment model as well as on Patlak analysis. Furthermore, parametric Patlak images have been calculated.

Visual analysis

Qualitative analysis of the 'late' PET/CT images was based on visual assessment of the static PET/CT scans acquired approximately 60 min post injection (p.i.). Areas presenting with significantly enhanced ^{68}Ga-PSMA-11 uptake in the prostate fossa, apart from those in which an increased tracer uptake is considered physiological, were considered positive for local PC recurrence. Qualitative evaluation of the early dynamic PET images was performed using the software package PMOD (PMOD Technologies Ltd, Zürich, Switzerland) [14, 15]. In particular, clearly delineated areas of increased tracer accumulation in the prostate fossa higher than background activity, were considered positive for local PC recurrence. The frame in which these lesions as well as urinary bladder were clearly detected was evaluated.

VOI-based analysis

Semi-quantitative evaluation was based on VOIs and on subsequent calculation of SUV values. VOIs were drawn with an isocontour mode (pseudo-snake) and were placed over the sites of local PC recurrence [16]. SUV values were calculated at the end of the dynamic PET acquisition (55-60 min p.i.).

The quantitative evaluation of the dynamic PET data was performed with PMOD software (PMOD Technologies Ltd, Zürich, Switzerland) and based on irregular VOIs placed over sites of local PC recurrence. The kinetics of ^{68}Ga-PSMA-11 can be described with a two-tissue compartment model, which reflects internalization of the receptor-ligand complex [11-13]. For the

Table 1. Characteristics of the patients investigated in the study

Patient number	Age	PSA	Gleason score	Previous therapy	Other metastases	Therapy change after imaging	$SUV_{average}$	SUV_{max}	Slope	Intercept
1	72	1.86	8	Radical prostatectomy and radiation therapy	Yes (bone)	Yes (radiation therapy and androgen deprivation therapy)	6.2	7.5	Positive	Positive
2	76	2.35	6	Radical prostatectomy and radiation therapy	No	Yes (Salvage-HIFU)	4.6	4.7	Positive	Positive
3	70	0.27	7	Radical prostatectomy and lymphadenectomy	Yes (lymph nodes)	Yes (Salvage radiation therapy to the prostatic fossa and pelvic nodes)	45.8	50.9	Positive	Positive
4	57	1.98	Unknown	Radical prostatectomy	No	Yes (8 months later radiation therapy by persistent PSA increase; no other imaging after ^{68}Ga-PSMA PET/CT)	10.7	12.3	Positive	Positive
5	72	2.00	9	HDR brachytherapy	Yes (lymph nodes)	Yes (TURP after 6 months; no other imaging after ^{68}Ga-PSMA PET/CT)	6.4	7.4	Positive	Positive
6	77	19.90	7	HIFU	Yes (lymph nodes, bone)	Yes (androgen deprivation therapy)	5.2	5.5	Positive	Positive
7	67	6.77	8	Radiation therapy	No	No	7.9	10.2	Positive	Positive
8	59	7.18	Unknown	Radiation therapy	No	No	3.1	3.3	Positive	Positive
9	69	1.20	9	Radiation therapy	No	Yes (Salvage-HIFU)	29.8	37.6	Positive	Positive
10	64	3.40	7	Radiation therapy	No	Yes (Salvage-HIFU)	12.7	13.1	Positive	Positive
11	60	Unknown	Unknown	Radical prostatectomy	Local recurrence is static PET/CT-negative and MRI-positive. No other lesions	Yes (Salvage radiation therapy)	n.a.	n.a.	Negative	Negative
12	68	4.17	Unknown	Radical prostatectomy and HIFU	No	Yes (HIFU)	26.5	29.0	Positive	Positive
13	69	11.66	7	Radical prostatectomy	Yes (lymph nodes)	Yes (androgen deprivation therapy after 9 months; no other imaging after ^{68}Ga-PSMA PET/CT)	14.5	27.2	Positive	Positive
14	73	4.60	7	Radical prostatectomy	Local recurrence is static PET/CT-negative and MRI-positive. No other lesions	Yes (androgen deprivation therapy; radiation therapy recommended, but declined from the patient)	n.a.	n.a.	Negative	Negative
15	78	2.02	9	Radical prostatectomy	Local recurrence is static PET/CT-negative and MRI-positive. Lymph nodes and bone metastases	Yes (androgen deprivation therapy)	n.a.	n.a.	Negative	Negative
16	71	0.18	10	Radical prostatectomy and lymphadenectomy	Local recurrence is static PET/CT-negative and MRI-positive. Lymph nodes and bone metastases	Yes (radiation therapy and androgen deprivation therapy)	n.a.	n.a.	Negative	Positive

HDR, high-dose rate; HIFU, High intensity focused ultrasound; TURP, transurethral resection of the prostate; n.a., not applicable.

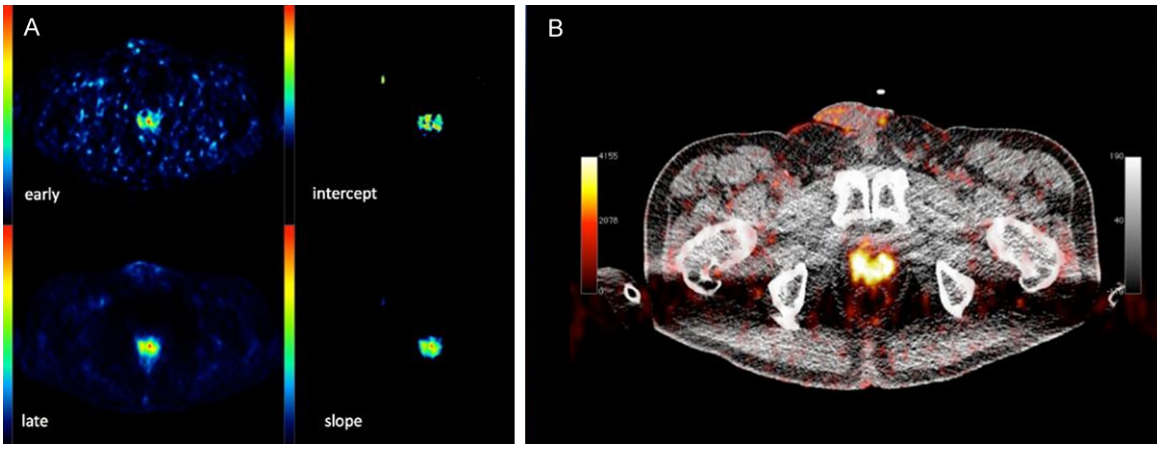

Figure 1. ^{68}Ga-PSMA-11 PET/CT of a 67-year-old patient with biochemical recurrence of PC (PSA at 6.77 ng/ml) attributed to local recurrence. A. Shows increased ^{68}Ga-PSMA-11 accumulation in the prostate fossa in the early dynamic image 7 min p.i. (upper left image, 'early'), which corresponds to the lesion depicted with increased tracer uptake in the late static image 60 min p.i. (lower left image, 'late'). High signal in the area of the local recurrence both in the intercept (upper right image, 'intercept') and the slope (lower right image, 'slope') parametric Patlak-based images. B. Exhibits the PC local recurrence seen as a pathological ^{68}Ga-PSMA-11 accumulation in the fused PET/CT image at 60 min p.i.

input function the mean value of the VOI data from the common iliac artery was used [17]. A vessel VOI consisted of at least seven consecutive regions of interest (ROIs). The recovery coefficient was 0.85 for a diameter of 8 mm. The application of two-tissue compartment modelling leads to the extraction of the parameters K_1, k_2, k_3 and k_4. Following compartmental analysis, we calculated the global influx (K_i) from the compartment data using the formula: $K_i = (K_1 \times k_3)/(k_2 + k_3)$.

The dynamic PET data (0-60 min p.i.) were also analysed with the Patlak plot model [18]. The Patlak plot is given by the expression:

$$\frac{C_{Tissue}(t)}{C_P(t)} = K\frac{\int_0^t C_P(\tau)d\tau}{C_P(t)} + V$$

where $C_{Tissue}(t)$ is the tissue concentration of the tracer at time t, $C_P(t)$ is the plasma concentration of the tracer at time t, K_{Patlak} (slope) is the tracer blood-tissue transfer constant and V_{Patlak} (intercept) equals V_0 + vB with the distribution volume V_0 of the reversible compartment and the fractional blood volume vB. As already mentioned, the input function was image-derived and generated from VOI data from the common iliac artery.

Parametric imaging

Parametric images of the slope and the intercept were calculated based on the dynamic PET data and after application of the PMOD software. These images were assessed visually and quantitatively by using the same VOIs drawn over sites of local recurrence as for SUV calculations: PC local recurrences with clearly enhanced signal in slope or intercept were classified as positive, while complete lack of enhancement in the recurrence area was classified as negative. The Patlak-based influx constant K_{Patlak} was calculated.

Statistical analysis

Data were statistically evaluated using the STATA/SE 12.1 (StataCorp) software on an Intel Core (2-3.06 GHz, 4 GB RAM) running with Mac OS X 10.8.4 (Apple Inc., Cupertino, CA, USA). The statistical evaluation was performed using descriptive statistics and Spearman's rank correlation analysis. The results were considered significant for P less than 0.05 ($P<0.05$).

Results

Visual analysis

Visual analysis of the static ^{68}Ga-PSMA-11 PET/CT scans acquired 60 min p.i. revealed that 12/16 patients were PET/CT-positive. The rest

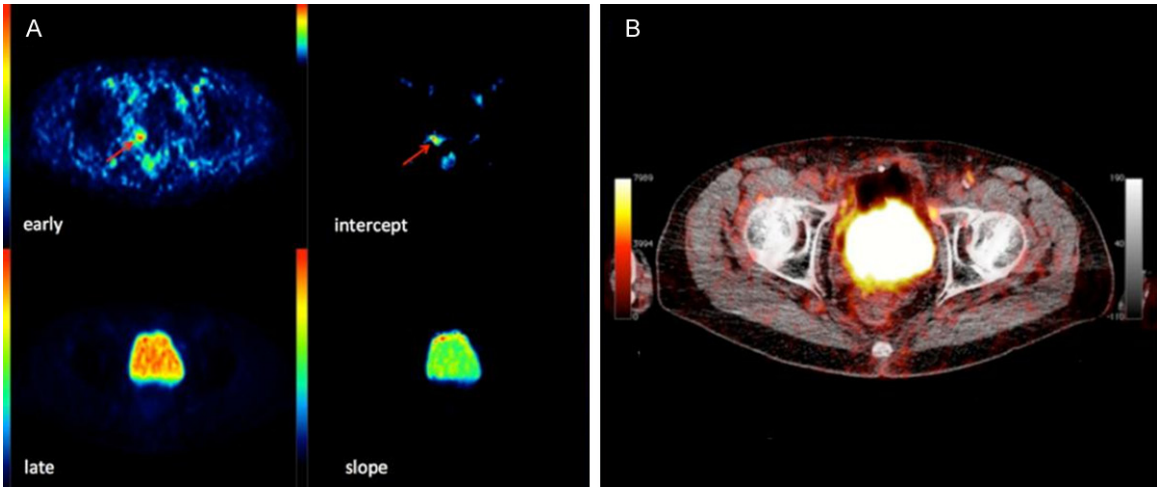

Figure 2. ^{68}Ga-PSMA-11 PET/CT of a 71-year-old patient with biochemical recurrence of PC (PSA at 0.18 ng/ml). A. Shows increased ^{68}Ga-PSMA-11 accumulation in the prostate fossa in the early dynamic image 6 min p.i. (arrow in the upper left image, 'early'), which is not observed in the late static image 60 min p.i., since it is 'masked' by the overlying bladder activity (lower left image, 'late'). High signal in the area of the local recurrence in the intercept (arrow in the upper right image, 'intercept') but not in the slope (lower right image, 'slope') parametric Patlak-based image. B. Exhibits no pathological ^{68}Ga-PSMA-11 accumulation in the fused PET/CT image at 60 min p.i.

Table 2. Descriptive statistics of VOI-based kinetic models parameters and semi-quantitative (SUV values) parameters

Parameters	Mean	Median	Minimum	Maximum
K_1	0.19	0.15	0.05	0.60
k_3	0.28	0.16	0.02	0.85
Influx-K_i	0.12	0.07	0.02	0.49
K_{Patlak}	0.11	0.08	0.02	0.32
$SUV_{average}$	13.7	7.9	3.1	45.8
SUV_{max}	16.6	10.2	3.3	50.9

The units of parameters K_1, k_3, influx-K_i and K_{Patlak} are 1/min. $SUV_{average}$ and SUV_{max} have no unit.

(4/16 patients) were negative on static PET/CT but positive on MRI. In 9 patients metastases in other sites (bone, lymph nodes) were also detected, while in 7 patients local recurrence was the only pathologic finding. Clinical follow-up was available in all patients. Patient management was altered in 14/16 patients based on imaging findings, while in 2 patients no therapy was initiated. All patients who received treatment demonstrated PSA-responses (**Table 1**).

Visual analysis of the early dynamic images showed that all 12 lesions corresponding to PC local recurrence could be detected in earlier frames of the dynamic PET acquisition at a median time of 4.5 min p.i. (range = 1.5-11.5 min) (**Figure 1**). Tracer accumulation in the urinary bladder began at a median time of 10 min (range = 6.0-17.5 min). No lesion detected on static PET/CT at 60 min p.i. was missed on early dynamic imaging. Moreover, early dynamic PET imaging could detect local recurrence in 1/4 patients who were negative on static PET/CT; this lesion was masked in the late/static images from bladder activity (**Figure 2**; **Table 1**).

VOI-based analysis

Descriptive statistics of the most important kinetic parameters (K_1, k_3 and influx-K_i) derived from two-tissue compartment model, the parameter K_{Patlak} derived from Patlak model as well as the $SUV_{average}$ and SUV_{max} are shown in **Table 2** as well as in **Figures 3** and **4**.

Quantitative analysis showed strong correlations between the Patlak-derived influx constant K_{Patlak} and the VOI-based influx-K_i calculated by the two-tissue compartment model ($r = 0.72$), as well as the $SUV_{average}$ ($r = 0.98$) and SUV_{max} calculated at 55-60 min p.i. ($r = 0.99$) (**Table 3**).

Parametric imaging

Parametric analysis revealed a positive signal in slope images in 12/16 local recurrences, and a positive signal in intercept images in 13/16 local recurrences (**Figure 1**). In particu-

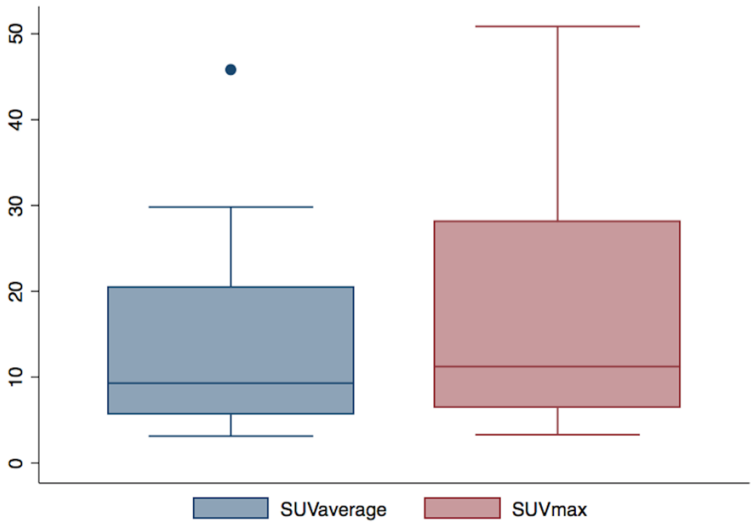

Figure 3. Box plots of the ^{68}Ga-PSMA-11 parameters $SUV_{average}$ and SUV_{max} in PC local recurrence lesions.

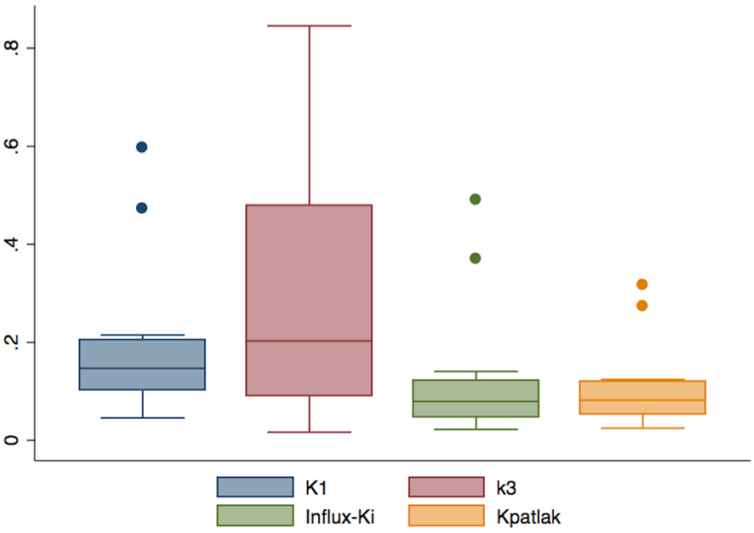

Figure 4. Box plots of the ^{68}Ga-PSMA-11 parameters K_1, k_3, influx-K_i and K_{Patlak} in PC local recurrence lesions.

lar, the Patlak graphic model showed that all late static PET/CT findings had a positive signal in slope images, but none of the 4 static PET/CT-negative lesions were slope-positive. On the other hand, intercept images were positive not only in the 12 PC local recurrence lesions, but also in the previously mentioned lesion only seen in the early dynamic images (**Figure 2**).

Discussion

According to the recently published Joint European Association of Nuclear Medicine and Society of Nuclear Medicine and Molecular Imaging procedure guidelines for ^{68}Ga-PSMA-11 PET/CT imaging, a 60-min interval p.i. is recommended for uptake time with an acceptable range of 50 to 100 min [19]. However, the physiologic accumulation of ^{68}Ga-PSMA-11 that takes place during this time period in the urinary bladder can hamper the detection of lesions in the pelvic region, rendering, thus, the visualization of PC local recurrences challenging [7]. Various methods have been proposed for reduction of radioactivity in the urinary bladder and, subsequently, better delineation of pathologic findings in the PET scans. Administration of furosemide is such a strategy, but the so far published results do not seem very encouraging [20, 21]. Another approach that has shown promising results is the acquisition of late PET/CT images at 180 min p.i. [20, 22]. However, this technique may be impractical, because it entails that the patient will spend much more time in the department and more scanning time is needed.

In view of this diagnostic challenge, we aimed to evaluate the potential complementary role of dynamic and parametric PET imaging for the detection of PC local recurrence. Our results showed that the application of early dynamic scanning led to the detection of a PC local recurrence in one patient, which would have been missed if only static PET/CT (60 min p.i.) was applied, due to high tracer accumulation in the urine. Moreover, all lesions depicted on static scans were visualized on the early dynamic PET imaging at a median time of 4.5 min p.i. and with a range of 1.5-11.5 min p.i. At that time point, no disturbing background activity from the urinary

Table 3. Results of the Spearman's rank correlation analysis between VOI-based kinetic models parameters and semi-quantitative (SUV values) parameters

	Influx-K_i	K_{Patlak}	$SUV_{average}$
K_{Patlak}	0.7203*		
$SUV_{average}$	0.7692*	0.9790*	
SUV_{max}	0.7552*	0.9860*	0.9930*

Values were considered significant for P<0.05. *Significant differences (P<0.05).

bladder was seen. Urinary bladder activity was demonstrated at a median time of 10 min.

These findings are in line with the results of Uprimny et al. who performed early static ^{68}Ga-PSMA-11 PET imaging of the pelvis starting at a median of 283 seconds p.i. (with a duration of PET emission of two min) as well as conventional late static PET imaging at 60 min p.i. in consecutive PC patients with biochemical failure. The authors showed that all patients judged positive for local recurrence on late PET/CT images were also positive on early PET/CT. Furthermore, early PET/CT resulted in a significant increase in detection rate of pathologic lesions in 24.6% of the studied patients [23]. The same group had performed early dynamic ^{68}Ga-PSMA-11 PET imaging of the pelvis in the first 8 min in a mixed group of PC patients with biochemical relapse and primary tumors. According to their results, median SUV_{max} of all tumor lesions in the time frames 1-6 min p.i. was significantly higher than in the urinary bladder [24]. Based on our and the previously mentioned findings, we suggest the acquisition of an early dynamic ^{68}Ga-PSMA-11 PET/CT scan of the pelvis up to 12 min p.i. in addition to the conventional PET/CT acquired at 60 min p.i.

We also applied Patlak analysis in the studied population in order to investigate the potential impact of parametric images in the evaluation of PC local recurrence. Although Patlak analysis is a pharmacokinetic approach used for dynamic ^{18}F-FDG PET studies, this graphical approach can also be used for tracers with irreversible uptake to describe pharmacokinetics. The assumption is that a radiotracer can be approximated by two tissue compartments, a reversible and an irreversible one. Parametric imaging is a method for feature extraction, enabling the visualization of single parameters of tracer kinetics. A pre-requisite for this analysis is dynamic PET acquisition. According to this model, the influx constant K_{Patlak}, which represents the tracer blood-tissue transfer constant, is obtained from the slope of the time-activity curve. We found that all PC lesions visible on late static ^{68}Ga-PSMA-11 PET/CT images were also positive both on the slope and the intercept Patlak images. Interestingly, the 'mismatch' lesion, which was positive in the early dynamic PET images but negative in the late static PET images, could be demonstrated on the intercept images. In contrary, it could not be delineated in the slope images since it was 'covered' by the urinary activity in the bladder. Thus, Patlak analysis, and in particular intercept images of the time-activity curve, may provide additional information in detection of PC local recurrence by means of ^{68}Ga-PSMA-11 PET/CT. However, the need for dynamic scanning during the whole time range of 60 min may be impractical in everyday clinical practice.

We have previously described the kinetics of ^{68}Ga-PSMA-11 by a two-tissue compartment model based on the assumptions mentioned before and found strong correlations between the global tracer influx K_i and the degree of tracer uptake, reflected by SUV [11, 12]. In the present study, very strong correlations were revealed between the Patlak-derived influx constant K_{Patlak}, obtained from the slope of the fit, the VOI-based influx K_i derived from two-tissue compartment model, as well as $SUV_{average}$ and SUV_{max}. These results come to support similar findings regarding the correlation of Patlak-derived influx K_{Patlak} and these parameters in patients with different tumors and studied with different tracers [25, 26].

However, our study has some limitations, the first one deriving from its retrospective nature. A prospective study is necessary to substantiate our findings. Another limitation is the relatively small number of patients enrolled. In addition, most PET positive findings were not validated histopathologically. However, personal communication either with referring physicians or the patients revealed that patient management was altered in 14/16 patients based on imaging findings, while in 2 patients no therapy was given. All patients who received treatment showed at least partial PSA decreases. Finally, we applied the Patlak and the two-tissue compartment models in order to describe

the ^{68}Ga-PSMA-11 distribution kinetics, although these are primarily used for the assessment of ^{18}F-FDG kinetics; however, both models have already been used for tracer kinetics evaluation of receptor-binding radioligands, as is the case for ^{68}Ga-DOTATOC and ^{68}Ga-DOTATATE [26].

Conclusions

In this study we could show that PC local recurrences could be detected in early frames of the dynamic ^{68}Ga-PSMA-11 PET/CT acquisition at a median time of 4.5 min p.i., while the ^{68}Ga-PSMA-11 accumulation in the urinary bladder began at a median time of 10 min. One lesion not seen on late static PET/CT images could be detected with early dynamic scanning. Therefore, a short data acquisition protocol including early dynamic scanning of the pelvis up to 12 min p.i., in combination with static, whole-body imaging at 60 min p.i. may be a good compromise to increase the detection rate of PC local recurrence. Patlak analysis, and in particular intercept images of the time-activity curve, may provide additional information in detection of PC local recurrence by means of ^{68}Ga-PSMA-11 PET/CT.

Disclosure of conflict of interest

None.

Address correspondence to: Dr. Christos Sachpekidis, Clinical Cooperation Unit Nuclear Medicine, German Cancer Research Center (DKFZ), Im Neuenheimer Feld 280, D-69120 Heidelberg, Heidelberg, Germany. E-mail: christos_saxpe@yahoo.gr

References

[1] Suardi N, Porter CR, Reuther AM, Walz J, Kodama K, Gibbons RP, Correa R, Montorsi F, Graefen M, Huland H, Klein EA, Karakiewicz PI. A nomogram predicting long-term biochemical recurrence after radical prostatectomy. Cancer 2008; 112: 1254-1263.

[2] Cornford P, Bellmunt J, Bolla M, Briers E, De Santis M, Gross T, Henry AM, Joniau S, Lam TB, Mason MD, van der Poel HG, van der Kwast TH, Rouvière O, Wiegel T, Mottet N. eau-estro-siog guidelines on prostate cancer. part ii: treatment of relapsing, metastatic, and castration-resistant prostate cancer. Eur Urol 2017; 71: 630-642.

[3] Hoeks CMA, Barentsz JO, Hambrock T, Yakar D, Somford DM, Heijmink SW, Scheenen TW, Vos PC, Huisman H, van Oort IM, Witjes JA, Heerschap A, Fütterer JJ. Prostate cancer: multiparametric MR imaging for detection, localization, and staging. Radiology 2011; 261: 46-66.

[4] Beer AJ, Eiber M, Souvatzoglou M, Schwaiger M, Krause BJ. Radionuclide and hybrid imaging of recurrent prostate cancer. Lancet Oncol 2011; 12: 181-191.

[5] Eiber M, Maurer T, Souvatzoglou M, Beer AJ, Ruffani A, Haller B, Graner FP, Kübler H, Haberkorn U, Eisenhut M, Wester HJ, Gschwend JE, Schwaiger M. Evaluation of hybrid 68Ga-PSMA-ligand PET/CT in 248 patients with biochemical recurrence after radical prostatectomy. J Nucl Med 2015; 56: 668-674.

[6] Perera M, Papa N, Christidis D, Wetherell D, Hofman MS, Murphy DG, Bolton D, Lawrentschuk N. Sensitivity, specificity, and predictors of positive 68Ga-prostate-specific membrane antigen positron emission tomography in advanced prostate cancer: a systematic review and meta-analysis. Eur Urol 2016; 70: 926-937.

[7] Afshar-Oromieh A, Holland-Letz T, Giesel FL, Kratochwil C, Mier W, Haufe S, Debus N, Eder M, Eisenhut M, Schäfer M, Neels O, Hohenfellner M, Kopka K, Kauczor HU, Debus J, Haberkorn U. Diagnostic performance of 68Ga-PSMA-11 (HBED-CC) PET/CT in patients with recurrent prostate cancer: evaluation in 1007 patients. Eur J Nucl Med Mol Imaging 2017; 44: 1258-1268.

[8] Freitag MT, Radtke JP, Afshar-Oromieh A, Roethke MC, Hadaschik BA, Gleave M, Bonekamp D, Kopka K, Eder M, Heusser T, Kachelriess M, Wieczorek K, Sachpekidis C, Flechsig P, Giesel F, Hohenfellner M, Haberkorn U, Schlemmer HP, Dimitrakopoulou-Strauss A. Local recurrence of prostate cancer after radical prostatectomy is at risk to be missed in 68Ga-PSMA-11-PET of PET/CT and PET/MRI: comparison with mpMRI integrated in simultaneous PET/MRI. Eur J Nucl Med Mol Imaging 2017; 44: 776-787.

[9] Eder M, Schäfer M, Bauder-Wüst U, Hull WE, Wängler C, Mier W, Haberkorn U, Eisenhut M. 68Ga-complex lipophilicity and the targeting property of a urea-based PSMA inhibitor for PET imaging. Bioconjug Chem 2012; 23: 688-697.

[10] Eder M, Neels O, Müller M, Bauder-Wüst U, Remde Y, Schäfer M, Hennrich U, Eisenhut M, Afshar-Oromieh A, Haberkorn U, Kopka K. Novel preclinical and radiopharmaceutical aspects of [68Ga]Ga-PSMA-HBED-CC: a new PET tracer for imaging of prostate cancer. Pharmaceuticals (Basel) 2014; 7: 779-796.

[11] Sachpekidis C, Eder M, Kopka K, Mier W, Hadaschik BA, Haberkorn U, Dimitrakopoulou-Strauss A. (68)Ga-PSMA-11 dynamic PET/CT imaging in biochemical relapse of prostate cancer. Eur J Nucl Med Mol Imaging 2016; 43: 1288-1299.

[12] Sachpekidis C, Kopka K, Eder M, Hadaschik BA, Freitag MT, Pan L, Haberkorn U, Dimitrakopoulou-Strauss A. 68Ga-PSMA-11 dynamic PET/CT imaging in primary prostate cancer. Clin Nucl Med 2016; 41: e473-e479.

[13] Sachpekidis C, Bäumer P, Kopka K, Hadaschik BA, Hohenfellner M, Kopp-Schneider A, Haberkorn U, Dimitrakopoulou-Strauss A. 68Ga-PSMA PET/CT in the evaluation of bone metastases in prostate cancer. Eur J Nucl Med Mol Imaging 2018; 45: 904-912.

[14] Burger C, Buck A. Requirements and implementations of a flexible kinetic modeling tool. J Nucl Med 1997; 38: 1818-1823.

[15] Mikolajczyk K, Szabatin M, Rudnicki P, Grodzki M, Burger C. A Java environment for medical image data analysis: initial application for brain PET quantitation. Med Inform 1998; 23: 207-214.

[16] http://www.pmod.com/files/download/v31/doc/pbas/4729.htm.

[17] Ohtake T, Kosaka N,Watanabe T, Yokoyama I, Moritan T, Masuo M, Iizuka M, Kozeni K, Momose T, Oku S, et al. Noninvasive method to obtain input function for measuring tissue glucose utilization of thoracic and abdominal organs. J Nucl Med 1991; 32: 1432-1438.

[18] Patlak CS, Blasberg RG. Graphical evaluation of blood-to-brain transfer constants from multiple-time uptake data. Generalizations. J Cereb Blood Flow Metab 1985; 5: 584-590.

[19] Fendler WP, Eiber M, Beheshti M,Bomanji J, Ceci F, Cho S, Giesel F, Haberkorn U, Hope TA, Kopka K, Krause BJ, Mottaghy FM, Schöder H, Sunderland J, Wan S, Wester HJ, Fanti S, Herrmann K. 68Ga-PSMA PET/CT: joint EANM and SNMMI procedure guideline for prostate cancer imaging: version 1.0. Eur J Nucl Med Mol Imaging 2017; 44: 1014-1024.

[20] Rauscher I, Maurer T, Fendler WP, Sommer WH, Schwaiger M, Eiber M. (68)Ga-PSMA ligand PET/CT in patients with prostate cancer: how we review and report. Cancer Imaging 2016; 16: 14.

[21] Derlin T, Weiberg D, von Klot C, Wester HJ, Henkenberens C, Ross TL, Christiansen H, Merseburger AS, Bengel FM. 68Ga-PSMA I&T PET/CT for assessment of prostate cancer: evaluation of image quality after forced diuresis and delayed imaging. Eur Radiol 2016; 26: 4345-4353.

[22] Afshar-Oromieh A, Sattler LP, Mier W, Hadaschik BA, Debus J, Holland-Letz T, Kopka K, Haberkorn U. The clinical impact of additional late PET/CT imaging with 68Ga-PSMA-11 (HBED-CC) in the diagnosis of prostate cancer. J Nucl Med 2017; 58: 750-755.

[23] Uprimny C, Kroiss AS, Fritz J, Decristoforo C, Kendler D, von Guggenberg E, Nilica B, Maffey-Steffan J, di Santo G, Bektic J, Horninger W, Virgolini IJ. Early PET imaging with [68]Ga-PSMA-11 increases the detection rate of local recurrence in prostate cancer patients with biochemical recurrence. Eur J Nucl Med Mol Imaging 2017; 44: 1647-1655.

[24] Uprimny C, Kroiss AS, Decristoforo C, Fritz J, Warwitz B, Scarpa L, Roig LG, Kendler D, von Guggenberg E, Bektic J, Horninger W, Virgolini IJ. Early dynamic imaging in 68Ga-PSMA-11 PET/CT allows discrimination of urinary bladder activity and prostate cancer lesions. Eur J Nucl Med Mol Imaging 2017; 44: 765-775.

[25] Wu H, Dimitrakopoulou-Strauss A, Heichel TO, Lehner B, Bernd L, Ewerbeck V, Burger C, Strauss LG. Quantitative evaluation of skeletal tumours with dynamic FDG PET: SUV in comparison to Patlak analysis. Eur J Nucl Med 2001; 28: 704-710.

[26] Ilan E, Sandström M, Velikyan I, Sundin A, Eriksson B, Lubberink M. Parametric net influx rate images of 68Ga-DOTATOC and 68Ga-DOTATATE: quantitative accuracy and improved image contrast. J Nucl Med 2017; 58: 744-749.